

Available online at www.sciencedirect.com

Procedia Chemistry 3 (2011) 236–247

Chemistry
Procedia

22nd Solvay Conference on Chemistry

Modeling of photosynthetic light-harvesting: From structure to function

T. Renger

Johannes Kepler University Linz, Institute of Theoretical Physics, Altenberger Str. 69, 4040 Linz, Austria

Abstract

In order to bridge the gap between the crystal structure of photosynthetic pigment-protein complexes and the data gathered in optical experiments, two essential problems need to be solved. On one hand, theories of optical spectra and excitation energy transfer have to be developed that take into account the pigment-pigment (excitonic) and the pigment-protein (exciton-vibrational) coupling on an equal footing. On the other hand, the parameters entering these theories need to be calculated from the structural data. Good agreement between simulations and experimental data then allows to draw conclusions on structure-function relationships of these complexes and to make predictions.

In the development of theory, a delicate question is how to describe the interplay between the quantum dynamics of excitons and the dephasing of coherences by the coupling of excitons to protein vibrations. Quantum mechanical coherences are utilized for efficient light harvesting. In the reaction centers of purple bacteria an energy sink is created by a coherent coupling of exciton states to intermolecular charge transfer states. The dephasing of coherences can be monitored, e.g., by the temperature dependent shift of optical lines. In the Fenna-Matthews-Olson protein, which acts as an excitation energy wire between the outer chlorosome antenna and the reaction center complex, an energy funnel for efficient light-harvesting is formed by the pigment-protein coupling. The protein shifts the local transition energies of the pigments, the so-called site energies in a specific way, such that pigments facing the reaction center are redshifted with respect to those on the chlorosome side. In the light-harvesting complex of higher plants an excitation energy funnel is created by the use of two different types of chlorophyll (Chl) pigments, Chl*a* and Chl*b* and by the pigment-protein coupling that creates an energy sink at Chl*a* 610 located in the stromal layer at the periphery of the complex. The close contact between Chl*a* and Chl*b* gives rise to ultrafast subpicosecond exciton transfer, whereas dynamic localization effects are inferred to lead to long ps relaxation times between the majority of Chl*a* pigments.

Keywords: exciton transfer, dynamic localization, Fenna Matthews Olson protein, LHCI, bacterial reaction center, site energy funnel

1. Introduction

Nature has found a way to convert and store the energy of sun light into chemical energy, in a reaction scheme termed photosynthesis. It has been one of the most important questions in biology, chemistry and biophysics to unravel the molecular details of this reaction. The application of time-resolved optical spectroscopy in the investigation of the primary reaction of photosynthesis, pioneered independently by H. T. Witt [1, 2], L. Duysens [3] and B. Kok [4] in the 60's of last century, allowed them to establish a scheme of oxygenic photosynthesis that consists of two photosystems working in series. Photosystem II (PS-II) uses the light energy to split water into molecular oxygen, the basis of aerobic life on earth, into protons and into electrons. The latter are shuttled to photosystem I and used there to store light energy in the reductive power of NADPH. The light induced electron transfer and subsequent protolytic

reactions generate a transmembrane electrochemical potential difference of protons (proton motive force) that drives ATP synthesis.

Another major breakthrough in the unraveling of molecular mechanisms of photosynthesis came with the structural analysis of photosynthetic pigment-protein complexes by X-ray diffraction crystallography. The first crystal structure of a photosynthetic pigment-protein complex was obtained by the work of Fenna, Matthews and Olson [5, 6] on a protein that is called now the Fenna-Matthews-Olson protein. It acts as an excitation energy wire in green sulfur bacteria, connecting an outer antenna system to the reaction center. The first successful attempt to crystallize a membrane bound pigment-protein complex and analyze its structure in atomic detail was achieved by J. Deisenhofer, R. Huber, and H. Michel on the anoxygenic photosynthetic reaction center of purple bacteria [7]. Whereas there is a large diversity in the structure of light-harvesting antennae in different photosynthetic organisms, the pigment organization in the reaction centers are rather similar. A common feature is the arrangement of cofactors in two nearly symmetric branches that start from a central (bacterio) chlorophyll dimer known as the special pair, which acts as primary electron donor in purple bacteria.

The same type of pigments that transfer electrons in the reaction center collect the light in light-harvesting antennae and transfer the excitation energy to the reaction center. At low light intensities, the quantum efficiency of the transfer is close to 100 %, i.e., nearly each of the absorbed photons reaches the reaction center and leads to a charge separated state [8]. At high light intensities the reaction center is protected by regulation mechanisms that lead to a quenching of the excitation energy in the antenna (e.g., Ref. [9] and references therein). With femtosecond optical spectroscopy it became possible to study the kinetic details of the light-harvesting reaction in isolated antenna and reaction center complexes [10, 11]. In such experiments, the pigment-protein complexes are excited with a femtosecond optical pulse. The relaxation of the excitation energy is then probed by a second femtosecond pulse as a function of the delay time between the two pulses and the energy of the probe pulse. Due to the short pulse width of the optical pulses coherent superpositions of different excited electronic states can be created and the decoherence of such wavepackets induced by the pigment-protein coupling analyzed. The first report of such excitonic wavepackets came from transient absorbance anisotropy measurements at 10 K on the FMO-protein by Savhikin *et al.* [12]. An independent theoretical prediction of this effect was given [13].

In more advanced setups, a train of multiple pulses is used as in the newly developed two-dimensional Fourier transform electronic spectroscopy pioneered by Graham Fleming and coworkers [14]. This technique has succeeded to visualize excitonic coherences in different light-harvesting and reaction center complexes even at physiological temperature [15, 16] and for weak excitonic couplings [16]. An independent theoretical prediction of the presence of excitonic coherences at room temperature was given also [17]. The new experimental technique allows us to take a glimpse at the elementary quantum mechanical processes and the transition from quantum mechanic wave-like to classical point-like motion in excitation energy transfer reactions.

A challenging task for theory is to relate the spectroscopic information to the crystal structure of the complexes [18]. This task on one hand requires a dynamical theory that takes into account the pigment-pigment coupling and the pigment-protein coupling to derive equations of motion for the dynamical variables. Standard theories exist, if one of the two couplings dominates. If the pigment-pigment coupling is strong, the excited states of the pigments will be delocalized and exciton relaxation between these states can be described by multi-level Redfield theory. For strong pigment-protein coupling localized excited states will be excited in the antenna and the hopping like transfer of the excitation energy is described by Förster theory [19]. In most photosynthetic pigment-protein complexes, however, both types of couplings are of equal strength. A complete delocalization of excited states would not allow excitation energy transfer in a certain direction, that is, towards the reaction center. A complete localization of excited states, on the other hand, would lead to less efficient transfer because excitations could more easily get trapped. It is a challenge for theory to describe the intermediate regime where neither of the two types of couplings is weak. Important steps towards a nonperturbative theory including both couplings were taken by the development of modified Redfield theory [20, 21, 22] and generalized Förster theory [23, 24, 25, 26]. Modified Redfield theory, in which a basis of delocalized excited states is used, contains a non-perturbative description of the diagonal part of the exciton-vibrational coupling in that basis. In this way it includes multi-vibrational quanta transitions in the dissipation of excess energy of the excitons by the protein [21, 27]. Localization effects of the excitonic states caused by static disorder and different local transition energies (site energies) of the pigments are included in the definition of the exciton states. However, a dynamical localization of the exciton wavefunction is still neglected. That is, if two pigments have the same site energy, but only a very weak excitonic coupling, their excited states will be assumed to be delocalized, whereas in reality,

the exciton-vibrational coupling would dephase any coherences and thus would localize these states. To include such a dynamical localization requires a non-perturbative description also of the off-diagonal part of the exciton-vibrational coupling. In principle, the hierarchical equation of motion approach [17] contains such a description, at the expense of a large numerical effort.

An alternative way to deal with this problem is to introduce domains of strongly coupled pigments and to use a delocalized basis only for the excited states of those pigments that are in the same domain [28, 26]. Excitation energy transfer between different exciton domains is then described by generalized Förster theory, whereas modified Redfield theory can be applied to describe exciton relaxation within the domains. At present such a combination of theories is practically the only way to study excitation energy transfer in large pigment-protein complexes like the core complexes of photosystem I [28] and photosystem II [26], or LHC-II trimers [11, 29]. A conceptual difficulty is the definition of the domains of strongly coupled pigments. Usually, a cutoff value V_c is defined and only those pigments that are coupled to at least one other pigment of an exciton domain by an excitonic coupling that is larger than V_c are included in that domain. V_c should be in the order of the reorganization energy of the exciton-vibrational coupling in order to describe dynamic localization effects implicitly. Of course, an explicit inclusion would be desirable. Further below, we will discuss a simple model that was used to investigate the temperature-dependent localization of a mixed excited/charge transfer state of the special pair of the reaction center of purple bacteria [30].

A question, related in spirit, concerns the inclusion of high-frequency intramolecular vibronic transitions of the pigments into a lineshape theory of multi-pigment protein complexes. For a two-level system, representing a single pigment in a protein, these transitions may just be included in the spectral density of the exciton-vibrational coupling [31]. However, for an exciton domain containing a number of strongly coupled pigments such a procedure would imply that not only the electronic transitions delocalize but also the vibronic transitions involving excited intramolecular vibrational states. However, the related Franck-Condon factors are very small (< 0.1) [32] and, therefore, the respective excitonic couplings are weak compared to the exciton-vibrational coupling. Along these lines, it seems to be the most reasonable approach to take into account delocalization of excitonic states only between 0-0 transitions and to use a localized basis for the vibronic transitions involving excited intramolecular vibrational states [29].

Besides a dynamic theory of excitation energy transfer and optical spectra, a full comprehension of structure-function relationships requires a structure-based calculation of the parameters of the theory. Two important parameter classes are the excitonic couplings between pigments and their site energies, defined as the local transition energies at which the pigments would absorb if there was no excitonic coupling. Concerning the calculation of excitonic couplings, two principal problems are (i) the validity of the widely used point-dipole approximation and (ii) the inclusion of screening and local field effects caused by the electronic polarizability of the protein/solvent environment [33, 34, 35]. We have developed a method that can quantitatively account for these effects [33, 35]. In this Poisson-TrEsp method the electrostatic potential of the transition density of a pigment type calculated by an *ab initio* method in vacuum is fitted by atomic partial charges. The charges are rescaled to yield the vacuum transition dipole moment that can be estimated from the oscillator strength of the pigment in different solvents [36]. These charges are placed in molecule shaped cavities of the pigments in the protein. The protein environment is described by a homogeneous dielectric with optical dielectric constant of two that was estimated from optical properties of protein bound pigments and pigments in solution [18]. The electrostatic potential of a set of molecular transition charges is then obtained from the solution of a Poisson equation and from this potential the intermolecular Coulomb couplings between the transition charges, that is, the excitonic coupling results. Application to different systems [35, 37, 38] shows that in general the screening/local field effects can be well approximated by rescaling the vacuum couplings by a constant factor f that is somewhat system-dependent but in general in the range of $0.7 \dots 0.8$. The point-dipole approximation was found to be valid in the FMO-protein [33, 39, 35] and the LHCII [38] but it fails in photosystem I [37].

The molecular details of the tuning of site energies of the pigments are not easy to decipher. There are multiple interactions that influence the site energies, as interactions with charged amino acid residues ([40, 41]), hydrogen bonds between the pigment and the protein ([42, 43]), changes in the conformation of the pigments induced by the protein environment ([44]), interaction with the axial ligands ([45, 33]), and interaction with the neutral charge density of the protein and the other cofactors ([39, 35]). The complexity of the pigment-protein coupling and the many degrees of freedom of the protein are a challenge for any structure based calculation of site energies ([44, 41, 33, 39, 46, 35]).

Therefore, these site energies were often treated as free parameters that are determined from a fit of the optical experiments (e.g. [47, 48, 49, 50, 51, 52, 53, 54, 26]). The excitonic coupling between the pigments, however, makes a straightforward assignment of the bands of an optical spectrum to single pigments impossible because of partial

delocalization of electronic excitations. Therefore, a fit represents a highly non-linear optimization problem that involves the diagonalization of a matrix containing the site energies E_m in the diagonal and the excitonic couplings V_{mn} in the off-diagonal. The eigenvalues \mathcal{E}_M of this matrix determine the position of optical bands and from the eigenvectors $\mathbf{c}^{(M)}$ and the local transition dipole moments of the pigments the intensities of the absorbance bands are obtained (e.g. [31]). For larger complexes as photosystem I or photosystem II core complexes, containing 96 and 35 Chl a pigments, respectively, an unambiguous determination of the site energies from a fit of optical spectra becomes hopeless. In addition, the knowledge of the value of a site energy, even if it is true, still does not allow to draw conclusions about the microscopic mechanisms that lead to this value.

A promising methodology for a direct calculation of site energies was developed recently [39], using a combination of quantum chemical description of the pigments in vacuum with an electrostatic calculation of the whole pigment-protein complex in atomic detail, including also a thermal average over the protonation probabilities of titratable amino acid residues. In this approach, the site energies are obtained as

$$E_m = E_0 + \Delta E_m, \quad (1)$$

where E_0 is a single parameter and the relative site energy shifts ΔE_m are obtained from the quantum chemical/electrostatic calculations. The latter provide the charge densities of the ground and excited states of the pigments. The resulting electrostatic potentials are fitted by atomic partial charges that are used afterwards in electrostatic free energy calculations, including the whole pigment-protein complex in atomic detail. The method has been successfully applied to the FMO-protein [39] and the LHC-II [38]. In an effort to simplify the approach of [39], a method was developed ([35]), in which the polarization of the protein is described by an effective dielectric constant ϵ_{eff} . In this so-called charge density coupling (CDC)-method, the site energy shifts ΔE_m are obtained as

$$\Delta E_m = \frac{1}{\epsilon_{\text{eff}}} \sum_j \Delta \phi_m(\mathbf{r}_j) q_j, \quad (2)$$

where $\Delta \phi_m(\mathbf{r}_j)$ is the difference in electrostatic potential between the excited and the ground state of pigment m , shown for bacteriochlorophyll a in Fig. 1, and q_j are atomic partial charges of the remaining parts of the pigment-protein complex, that are based on fits of the electrostatic potential of the electronic ground state and are obtained from standard molecular mechanics force fields.

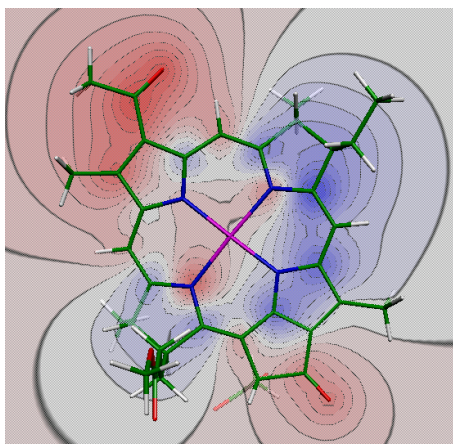


Figure 1: Difference in electrostatic potential $\Delta\phi$ between the charge densities of the excited and the ground state of BChla obtained with time-dependent density functional theory using the B3LYP XC functional [55]. The regions in red (blue) have $\Delta\phi < (>)0$.

The difference potential in Figure 1 suggests that upon electronic excitation the electrons tend to move from the blue regions into the red regions of $\Delta\phi$ shown in Figure 1. By placing appropriate charges into the environment of the pigments, the protein can stabilize/destabilize the electronic states of the pigments thereby tuning the transition energies (site energies). Further below we will discuss the molecular details of such a tuning that leads to an excitation

energy funnel in the FMO protein. The CDC method indeed provided similar site energies ([35]) as the more elaborated method of Ref. [39]. The former has been also applied to photosystem I [37] revealing a higher concentration of low energy exciton states on that side of the antenna that is connected to the A-branch of the reaction center, which is used more frequently than the B-branch in electron transfer reactions. The calculations also demonstrated the importance of long-range electrostatic effects explaining why earlier purely quantum chemical approaches [56, 46] gave less accurate results. Finally, we note that the CDC method was originally applied by assuming a standard protonation pattern of the protein [35], but it was later extended to include a thermodynamic average over the protonation probabilities of titratable amino acid residues [37, 57]. In photosystem I a critical amino acid was indeed found in a non-standard protonation state [37].

The remaining part of this paper is organized in the following way. We first discuss two different strategies to create an excitation energy funnel, which are realized in purple and sulfur bacteria. In purple bacteria this funnel will lead us to a mixed excited/charge transfer state in the special pair that is the ultimate sink of the excitation energy. We will discuss a simple model that can describe the temperature dependent dephasing of this quantum mechanic coherence, a phenomenon that is seen in the experiment as a 30 nm blueshift of the absorbance band, when temperature is varied between 15 K and room temperature. Next, the site energy funnel realized in the FMO-protein of green sulfur bacteria will be discussed with special emphasis on structure-function relationships. Finally, we discuss light-harvesting in the major antenna of higher plants, LHCII. In this case the focus will be on energy sinks as revealed from structure-based calculations. An application of generalized Förster theory is presented which implicitly takes into account dynamic localization effects of excited states. This theory allows to describe the slow exciton relaxation detected experimentally in the Chl*a* spectral region. Finally, we discuss challenges for the modeling of light-harvesting that need to be addressed in the future.

2. Two different types of excitation energy funnels in bacteria

2.1. *The excitonic/charge transfer interaction funnel in purple bacteria*

Nature has chosen different strategies to create efficient energy transfer pathways. In purple bacteria the inter-pigment coupling is used to form an excitation energy funnel within the outer LH2 ring-shaped antenna system and between the latter and the inner LH1-ring surrounding the photosynthetic reaction center ([58]). The LH2-complex contains a ring of 18 strongly coupled BChl*a* pigments absorbing light at 850 nm and another ring of 9 weakly coupled BChl*a* pigments that absorb at 800 nm. A large part of the shift in absorbance from 800 to 850 nm is due to the excitonic coupling that delocalizes the excited states of the strongly coupled BChls. This delocalization results in a shift of the excited state energies of the coupled BChls and in a redistribution of their oscillator strengths among the different delocalized excited states, the so-called exciton states. From the exciton states at 850 nm in LH2 the excitation energy is transferred to the LH1 ring that absorbs at 875 nm, i.e. even further red-shifted. This shift results from an increased number (32) of strongly coupled pigments in LH1. From the exciton states in LH1 the excitation energy is finally trapped by the special pair in the photosynthetic reaction center, absorbing around 860 nm.

The question arises why 32 pigments are needed to shift the absorbance from 800 nm for monomeric BChl in LH2 to 875 nm for the low energy exciton states in LH1 and only 2 pigments to obtain a 60 nm redshift in the special pair of the reaction center? The answer lies in the very small distance between the two special pair pigments. Due to their wavefunction overlap those two pigments cannot only exchange excitation energy but also electrons. This short-range coupling further lowers the excited state energies ([59, 30]). The origin of this additional shift is on one hand a short-range contribution to the excitonic coupling [60], and on the other hand a coupling between the exciton states and intramolecular charge transfer states ([59, 61]) that shifts the energies of the dimer and also contributes to the excitonic coupling. Theoretical methods have been developed to decipher the short-range effects from quantum chemical calculations. The idea is to relate the results of quantum chemical calculations of the isolated monomers to those calculated for the dimer by using an effective two state Hamiltonian [62, 63]. If, in addition to the excitation energies, also the transition dipole moments are taken into account, the number of unknowns is smaller than the number of equations. Therefore it becomes possible to use part of the equations to calculate the short-range site energy shifts and excitonic coupling and the remaining equations to check for the consistency of the approach and on this basis to provide an error estimate of the method [63]. An analysis of the special pair of purple bacteria reveals that indeed the short-range effects are responsible for its low excitation energy [63].

Additional spectroscopic signatures for the coupling of exciton states with charge transfer states, besides the strong redshift, are the appearance of optical transitions with strong vibrational sidebands, strong Stark signals, and strong pressure shifts. Optical spectroscopy on bacterial reaction centers [64, 65, 66] prompted theoretical investigations on the role of intradimer charge transfer states of the special pair [59, 67, 68, 30]. The absorption of a three electronic state system, was studied by Lathrop and Friesner [67] using a Greens function approach that takes into account a few explicit vibrational degrees of freedom and uses a damping parameter to describe the remaining vibrational modes. A different approach was chosen by Zhou and Boxer [68] who applied a Fano type theory [69] to describe the coupling of a discrete excited state to a continuum of vibrational levels of the charge transfer state. Whereas the latter theory [68] does not contain the temperature dependence of the spectra the former [67] takes into account the continuum of low frequency vibrational modes by a single damping parameter. A multi-mode theory, using a spectral density to describe the coupling of a three electronic state system to a vibrational continuum was investigated also [30]. This theory represents an instructive example of how the coupling of a quantum system to an environment can destroy the electronic coherence in the system, as will be discussed in more detail in the following. The three states are an electronic ground state g , an excited state e and a charge transfer state c . Harmonic potential energy surfaces (PES) are assumed for these three states. For simplicity we assume that the PES of e and g are unshifted (along the many vibrational coordinates) with respect to each other and the PES of c is strongly shifted because of the polar nature of c . In addition, we assume that the transition dipole moment of $g \rightarrow c$ is zero, i.e. c is optically dark but, due to an electronic coupling V_{ec} between e and c may borrow oscillator strength from the $g \rightarrow e$ transition that has a non-zero transition dipole moment. The equations of motion for the density matrix element ρ_{eg} , relevant for the calculation of linear absorbance,

$$\frac{d}{dt}\rho_{eg}(t) = -\frac{i}{\hbar}E_e\rho_{eg}(t) - \frac{i}{\hbar}V_{ec}\rho_{cg} \quad (3)$$

is coupled to density matrix element ρ_{cg} describing the polarization between the ground and the charge transfer state, for which the following equation of motion is obtained

$$\frac{d}{dt}\rho_{cg}(t) = -i\{E_c/\hbar - \lambda + \Gamma(t)\}\rho_{cg}(t) - \frac{i}{\hbar}V_{ec}\rho_{eg}(t). \quad (4)$$

The time-dependent function $\Gamma(t)$ describes the dynamic modulation of the CT state energy by the vibrations. Neglecting a direct influence by the charge transfer coupling V_{ec} and using the time-local partial ordering prescription theory [70, 71, 27], $\Gamma(t)$ is obtained as

$$\Gamma(t) = \int_0^\infty d\omega J(\omega)\omega \left\{ (1 + n(\omega))e^{-i\omega t} - n(\omega)e^{i\omega t} \right\}, \quad (5)$$

with the spectral density $J(\omega)$ and the Bose-Einstein distribution function

$$n(\omega) = \frac{1}{e^{\hbar\omega/(kT)} + 1} \approx \exp\left\{-\frac{\hbar\omega}{kT}\right\} + \exp\left\{-2\frac{\hbar\omega}{kT}\right\} + \frac{kT}{\hbar\omega} \exp\left\{-\frac{5}{2}\frac{\hbar\omega}{kT}\right\}. \quad (6)$$

describing the mean number of vibrational quanta that are excited at a given temperature T . The λ in eq 4 is the reorganization energy $\lambda = \hbar \int d\omega \omega J(\omega)$. The Jang-Cao-Silbey approximation in the right part of Eq. 6 was found very helpful in the calculation of $\Gamma(t)$ in Eq. 5.

A critical parameter in the calculations is the energy difference $\Delta E_{ce} = E_c - E_e$ between the CT state and the excited state. Four different situations are discussed: a) $\Delta E_{ce} > \lambda_c$, b) $\Delta E_{ce} = \lambda_c$, c) $\Delta E_{ce} = 0$ and d) $\Delta E_{ce} < \lambda_c$. In Fig. 2 the absorbance, obtained from a half-sided Fourier transform of ρ_{ec} , is shown at different temperatures and for four different arrangements a) - d) of the PES of the charge transfer state $|c\rangle$. A coupling value $V_{ec} = 150$ meV was used in the numerical calculations and a shape of $J(\omega)$ extracted earlier [71]. The amplitude of $J(\omega)$ was rescaled such that a reorganization energy $\lambda = \hbar \int d\omega \omega J(\omega) = 0.2$ eV results, which is similar in magnitude to the electronic coupling V_{ec} . The high value of $T = 3000$ K was included because the resulting absorbance (thin dotted line) was found to resemble that obtained for uncoupled states ($V_{ec} = 0$).

Two main results of this model study are: (i) depending on the relative positions of PES of excited and charge transfer state, one or two absorption bands with strong vibrational sidebands appear in the spectrum at a given temperature, (ii) a temperature dependence of the band positions is found: with increasing temperature the bands move towards the

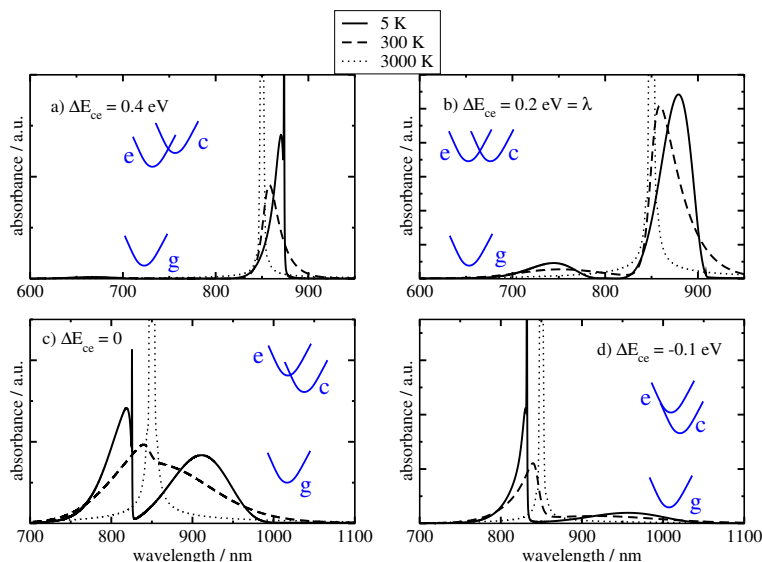


Figure 2: Absorbance spectra of a simple model system that contains a coupling between an optically excited state e and a dark charge transfer state c , in dependence on temperature and the energy difference between these two states, as illustrated in the insets.

single band that is obtained for absent coupling ($V=0$, the thin dotted line in Fig. 2). The coupling between states $|e\rangle$ and $|c\rangle$ leads to optical transitions that are shifted with respect to the transition for $V=0$ and contain vibrational sidebands. The optical bands contain the signature of the quantum mechanical mixing of the two states. Two effects of the mixing are that $|c\rangle$ borrows intensity from $|e\rangle$ and $|e\rangle$ borrows a vibrational sideband from $|c\rangle$. The relative strength of those effects in the spectrum depends on the energetics of the PES of the two states. For example, in case a) $\Delta E_{ce} > \lambda_c$ and $\Delta E_{ce} > V$, the resulting redistribution of oscillator strength is minor, and only one peak is seen in the spectrum, but this transition now contains a strong vibrational sideband and is red-shifted with respect to the transition of the uncoupled state $|e\rangle$. The intensity borrowing by the CT state has its maximum when the CT state PES crosses the PES of state $|e\rangle$ in the minimum position of the latter, in case c). When temperature is increased the intrastate dephasing becomes larger and thus disturbs the coherent mixture of the two states $|c\rangle$ and $|e\rangle$ resulting in a smaller splitting between the two optical transitions. For $\Delta E_{ce} > 0$ this effect leads to a blueshift and for $\Delta E_{ce} < 0$ to a redshift of the main band.

The present model of dynamic localization was used to explain [30] the 30 nm blue shift of the low energy special pair absorption band of photosynthetic reaction center of purple bacteria, observed [66] between 15 K and room temperature. The energetics of the PES of the excited state $|e\rangle$ and the CT state $|c\rangle$ resembles model case a) $\Delta E_{ce} > V$, $\Delta E_{ce} > \lambda_c$ studied in Fig. 2, supporting quantum chemical calculations [59, 63]. Finally, we note that an application of the present model to describe exciton transfer requires to take into account the coupling V_{ec} in the derivation of the dephasing terms, which was neglected so far.

2.2. The site energy funnel in the FMO protein

An alternative strategy to guide the excitation energy to the reaction center is to use the pigment-protein coupling for tuning the local optical transition energies of the pigments, the so-called site energies, in a specific way.

This second type of excitation energy funnel is realized in the Fenna-Matthews-Olson (FMO)-protein of green sulfur bacteria ([5, 72]). The FMO-protein, which functions as an excitation energy wire between the outer antenna system and the reaction center, is a homotrimer, where each monomer contains seven or eight excitonically coupled BChl a molecules. From scanning transmission electron microscopy [73] and linear dichroism studies [74] on super complexes of the FMO protein and the reaction center (RC) complex, it was known that the symmetry axis of the FMO trimer is oriented normal to the membrane containing the RC complex.

Since its crystal structure became published more than 30 years ago ([5]), many different sets of site energies were suggested in the literature, based on fits of optical spectra (e.g. [47, 48, 49, 13, 50, 33]). A large part of the puzzle

was solved by Aartsma and coworkers [49], who recognized that assuming a lower effective dipole strength of the optical transitions of the BChl_a pigments, leading to smaller excitonic couplings, allows one to find site energies that can describe the experimental absorbance, linear dichroism and circular dichroism spectra at low temperatures better than any other set of site energies suggested before. A quantitative explanation of the low effective dipole strength was provided recently from electrostatic calculations ([33]). Interestingly, the inclusion of vibrational sidebands, resonance energy transfer narrowing and lifetime broadening into the theory used for the fit of optical spectra resulted in very similar site energies ([33]) as the earlier fit [49], where these effects were neglected. From calculations of the excitation energy flow [33], it was concluded that, for efficient transfer to the RC, the orientation of the FMO protein should be such that the energy sink BChl 3 is the linker pigment to the RC, i.e., that the site of the FMO protein where BChl 3 is located faces the cytoplasmic membrane, and that the opposite orientation which would also be in agreement with the LD measurements, discussed above, is unlikely. Recently, this prediction was verified by a combination of chemical labeling and mass spectrometry by the Blankenship group [75].

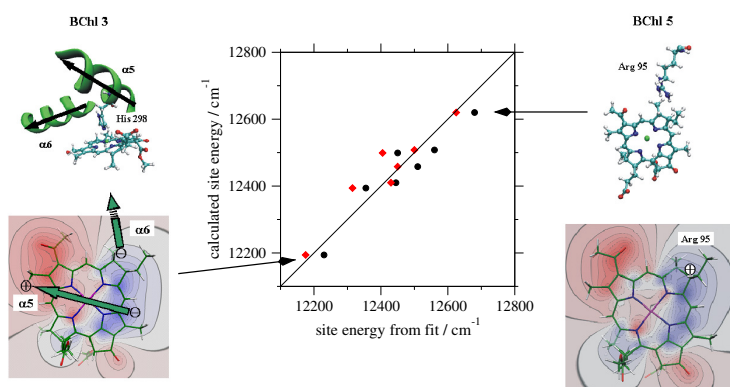


Figure 3: The middle part contains the correlation between site energies of the FMO protein obtained from two different fits [50, 33] of linear optical spectra and from direct structure-based calculations [39]. The upper parts on the left and the right show structural elements that have a strong influence on the site energies of BChl 3 and BChl 5. The respective lower parts locate the effective charges of these elements relative to the difference potential of the pigments.

In order to unravel the structure-function relationships of the site energy funnel realized in the FMO protein one has to identify the relevant molecular interactions. Site energies obtained by direct structure-based calculations describe the linear optical spectra quantitatively ([39]) and are similar to the fitted values [49, 33] discussed above, as shown in the correlation plot in Fig. 3. The calculated site energies revealed that the excitation energy sink at BChl 3 in the FMO protein is determined by the electric field of the backbone of two α -helices ([39]). The dipole moments of the two alpha helices are oriented such that the negative ends are located in the positive difference potential and one negative end is located in the positive difference potential of BChl 3 (Fig. 3). The high site energy of BChl 5 is caused by an Arg residues that is calculated to be in its standard protonation state, that is, positively charged. This charge is located in the positive difference potential of BChl 5 thereby causing the blueshift.

Surprisingly, recent crystallographic studies discovered an eighth BChl in each monomeric subunit of the FMO protein [76, 77]. This pigment is located in a cleft at the surface of the protein at the side of the baseplate which connects the outer antenna with the FMO protein. Therefore, it is likely that BChl 8 is the linker of the FMO protein to the baseplate [77]. Indeed, the site energy of this pigment was found [57] to be blueshifted with respect to the other pigments, still allowing for sufficient spectral overlap with the fluorescence spectrum of the baseplate for efficient excitation energy transfer. The blueshift of BChl 8, which is caused by interaction with negatively charged ASP and GLU residues at the surface of the protein, with respect to the energy sink at BChl 3 is about 400 cm^{-1} , that is two times the thermal energy at room temperature. We think that this large energy gap and the fast exciton equilibration in the FMO protein, which is completed in about 2-3 ps, lead to an efficient unidirectional excitation energy transfer from the outer antenna to the reaction center complex.

It would, of course, be desirable to obtain detailed structural information about the baseplate and reaction center environment of the FMO protein. With this information at hand it would be possible to give estimates for the relative

timescales of inter- and intraprotein excitation energy transfer. An interesting question would be whether the coherences found in the FMO protein [78, 15] survive the transfer between different proteins, and if so, how they influence the light-harvesting efficiency.

3. Light-harvesting in the major plant light harvesting complex LHCII

In higher plants, excitation energy funnels are created by the use of two different types of chlorophyll (Chl) pigments, Chl*a* and Chl*b* in the outer antennae and the use of only Chl*a* in the core complexes of photosystem I and photosystem II. The major light-harvesting complex in plants the trimeric LHC-II contains 6 Chl*b* and 8 Chl*a* per monomeric subunit [79, 80]. Except for one Chl*b* which is expected to form the bottleneck of the Chl*b* to Chl*a* transfer [81, 10, 11], all other Chl*b* pigments are in close contact with a neighboring Chl*a* pigment giving rise to ultrafast subpicosecond excitation energy transfer from the high to the low energy region that is on a wavelength scale from around 650 nm (Chl*b*) to 680 nm (Chl*a*). Chl*b* to *a* transfer times measured on LHCII trimers [82] (< 0.3 ps, 0.6 ps, 4-9 ps) are similar to those measured on LHCII monomers (200 fs, 3ps)[83]. It was more surprising that the slow 10-20 ps component in the Chl*a* spectral region assigned first to reflect excitation energy transfer between Chl*a* in different monomers [82] was also found in isolated monomers [84]. Mutant studies [85, 86], fitting of optical spectra [81, 10, 11] and a direct structure-based calculations of excitonic couplings and site energies [38] identified the energy sink of LHCII at Chl*a* 610 in the nomenclature of Ref. [79]. This Chl is situated in the stromal layer of pigments at the periphery of the LHCII trimer, that is, at an ideal position for excitation energy transfer to a neighboring light-harvesting complex.

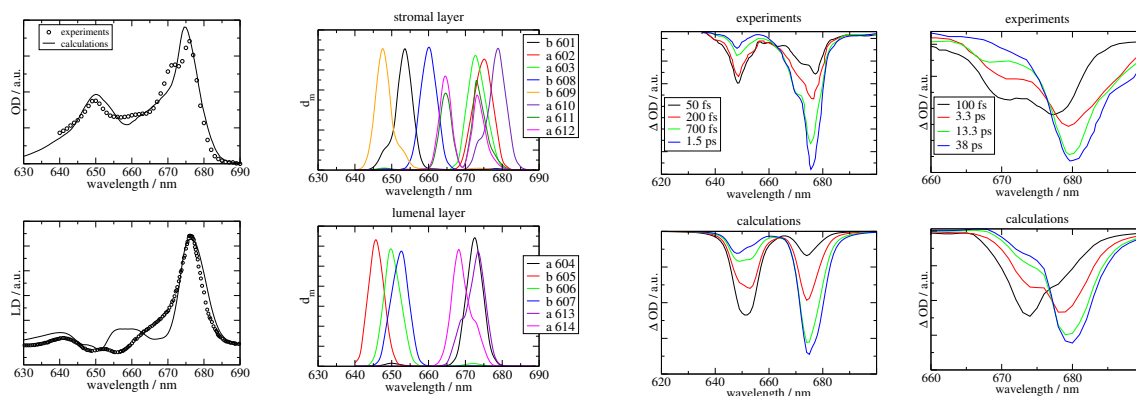


Figure 4: *Left part* compares experimental linear absorbance (OD) [87] and linear dichroism (LD) [88] spectra with calculations [29] using structure-based calculated site energies [38]. *Middle left part* shows the exciton state pigment distribution function $d_{m_i}(\omega) = \langle \sum_{M_i} |c_{m_i}^{M_i}|^2 \delta(\omega - \omega_{M_i}) \rangle_{dis}$ of the Chls in the stromal (top) and luminal (bottom) layer of LHC-II trimers. Exciton domains were defined with $V_c = 20 \text{ cm}^{-1}$, m_i counts the pigments in domain i and M_i the exciton states. *Middle right part* compares pump-probe spectra of LHC-II trimers measured [81] using an excitation with a 90 fs pump-pulse centered at 650 nm at 77 K (upper part) with calculations [29] (lower part). The *right part* shows pump-probe spectra of LHCII monomers excited with a 150 fs pump pulse at 669 nm at 77 K. The experimental data [84] are shown in the upper and the calculations [29] in the lower part.

A comparison between experimental linear absorbance and linear dichroism spectra at 4 and 77 K, respectively, with recent simulations [29] using structure-based calculated site energies and excitonic couplings [38] is shown in the left part of Fig. 4. The calculations, which use a theory of optical spectra that includes intramolecular vibronic transitions of the chlorophylls, agree semi-quantitatively with experiment. The calculations of pump-probe spectra for excitation in the Chl*b* region (650 nm) and excitation of the high-energy Chl*a* states (669 nm) reveals fast subpicosecond energy transfer from Chl*b* to Chl*a* and besides some subpicosecond component, slow ps energy transfer/equilibration times between the Chl*a* pigments, respectively in agreement with the experimental data [81, 84]. We note that the latter spectra were measured (and calculated) on LHC-II monomers. The calculations, which were performed by using generalized Förster theory, with a cut off coupling value $V_c = 20 \text{ cm}^{-1}$, for the definition of exciton domains correctly predict the long life times of Chl*a* exciton states. In this way, indirect evidence about the presence of dynamic localization effects of the exciton state wavefunction between weakly coupled pigments in different

domains is obtained. Earlier monomer calculations, which used modified Redfield theory and allowed for exciton delocalization between all pigments, obtained much shorter life times of these states and concluded that the only possible Chla bottleneck state is Chla 604 [81]. In the present calculations fast exciton relaxation occurs only within the terminal emitter domain formed by Chlsa 610,611,612 in the stromal layer and within the Chla 613/614 dimer in the luminal layer, whereas all other excitation energy pathways involving Chla pigments are slow. It would, of course be desirable to obtain the localization effects responsible for the slow relaxation times directly from the calculations, rather than to impose them by defining the exciton domains of generalized Förster theory. The hierarchical equation of motion approach [17] might be the right tool to reach this goal.

Finally we want to address some unresolved issue containing excited states of LHCII in the intermediate spectral region between Chla and Chlb around 660 nm. Excitation in this spectral region revealed slow 2-5 ps lifetimes [82, 84, 89, 90]. Novoderezhkin and van Grondelle identified Chlb 605 as the bottleneck state for the Chlb to *a* transfer and from fitting of optical spectra determined its site energy in the intermediate spectral region around 660 nm. In contrast, direct structure-based calculations of site energies obtained a site energy of Chlb 605 that places it at the blue edge of the Chlb spectral region around 647 nm, as seen in the exciton state pigment distribution function in Fig. 4. The only pigment absorbing around 660 nm reported in these calculations is Chlb 608 (Figure 4), which is part of a Chlb exciton domain in the stromal layer of pigments. However this pigment could not explain the long life times detected since it exhibits fast sub picosecond transfer to the neighboring Chla terminal emitter domain. Therefore besides this pigment another pigment so far not identified by the structure-based calculations should absorb in the intermediate spectral region. One possible candidate for such a state obviously is Chlb 605 [81]. Another candidate is Chla 604. From fitting of optical spectra it was concluded that this pigment absorbs at 667-672 and represents the bottleneck for exciton relaxation in the Chla spectral region [81]. However, taking into account dynamic localization effects many other slow pathways appear [29], as discussed above. Hence, Chla 604 could absorb slightly blueshifted without loosing the long lifetimes at longer wavelengths. The calculations of site energies [38] show that the excitation energy of Chlb 605 is influenced by Asp 111 and His 120, and that Tyr 112 has a strong influence on the site energy of Chla 604. Mutation of these residues could help to pinpoint the excitation energies of these putative bottleneck states. Other candidates are Chla 613 and 614 that were suggested by mutagenesis studies [85, 86].

4. Challenging problems to be solved in the future

The spectroscopic techniques, the structure analysis tools, the theory of optical spectra and the methodology for the calculation of parameters of the theory need to be developed further. Structural information on whole photosystems will allow us to study in detail how individual transfer steps contribute to the overall efficiency of light-harvesting. Techniques like 2D electronic spectroscopy are overwhelmingly rich in information and ways have to be found to extract it. A theory of optical spectra that includes both types of couplings, the excitonic and the exciton-vibrational, non-perturbatively, and is simple enough to be applied to whole photosystems shall be created. Such a theory should directly reveal dynamic localization effects of the excitonic wavefunction. A direct calculation scheme for the spectral density $J(\omega)$ characterizing the dynamic modulation of the transition energies of the pigments needs to be developed, most likely, by combining quantum chemical, electrostatic and molecular dynamics calculations. These calculations would also reveal the correlation in site energy fluctuations between different pigments, which is often neglected in the theories of energy transfer, but can be visualized with 2D electronic spectroscopy.

5. Acknowledgements

I would like to thank my coworkers Dr. El-Amine Madjet, Dr. Frank Müh, and Dr. Julian Adolphs. I am grateful to the German Research Foundation for generous support through Collaborative Research Centers 429 and 498, and through Emmy-Noether grant RE-1610.

6. References

- [1] H. T. Witt, A. Müller, B. Rumberg, *Nature* 191 (1961) 194.
- [2] H. T. Witt, A. Müller, B. Rumberg, *Nature* 197 (1963) 987.
- [3] L. N. M. Duysens, J. Amesz, B. M. Kamp, *Nature* 190 (1961) 510.

- [4] B. Kok, G. Hoch, Spectral changes in photosynthesis. In: McElroy, W. D. Glass, B. (eds) *Light and life.*, John Hopkins Press, Baltimore, 1961.
- [5] R. E. Fenna, B. W. Matthews, *Nature* 258 (1975) 573.
- [6] R. E. Blankenship, J. M. Olson, M. Mette, in: R. E. Blankenship, M. T. Madigan, C. E. Bauer (Eds.), *Anoxygenic photosynthetic bacteria*, Kluwer Academic Publishers, Dordrecht, Netherlands, 1995, p. 399.
- [7] J. Deisenhofer, O. Epp, K. Miki, R. Huber, H. Michel, *Nature* 318 (1985) 618.
- [8] R. van Grondelle, J. P. Dekker, T. Gillbro, V. Sundström, *Biochim. Biophys. Acta* 1187 (1994) 1.
- [9] A. V. Ruban, R. Berera, C. Illoaia, I. H. M. van Stokkum, J. T. M. Kennis, A. A. Pascal, H. van Amerongen, B. Robert, P. Horton, R. van Grondelle, *Nature* 450 (2007) 575.
- [10] V. I. Novoderezhkin, R. van Grondelle, *Phys. Chem. Chem. Phys.* 8 (2006) 793.
- [11] V. I. Novoderezhkin, R. van Grondelle, *Phys. Chem. Chem. Phys.* 12 (2010) 7352.
- [12] S. Savhikin, D. Brick, W. S. Struve, *Chem. Phys.* 223 (1997) 303.
- [13] T. Renger, V. May, *J. Phys. Chem. A* 102 (1998) 4381.
- [14] Y. C. Cheng, G. R. Fleming, *Annu. Rev. Phys. Chem.* 60 (2009) 241.
- [15] G. Panitchayangkoon, D. Hayes, K. A. Fransted, J. R. Caram, E. Harel, J. Wen, R. E. Blankenship, G. S. Engel, *Proc. Natl. Acad. Sci. U.S.A.* 107 (2010) 12766.
- [16] E. Collini, C. Y. Wong, K. E. Wilk, P. M. G. Curmi, P. Brumer, G. D. Scholes, *Nature* 463 (2010) 644.
- [17] A. Ishizaki, G. R. Fleming, *Proc. Natl. Acad. Sci. U.S.A.* 106 (2009) 17255.
- [18] T. Renger, *Photos. Res.* 102 (2009) 471.
- [19] T. Förster, *Ann. Phys. Leipzig* 2 (1948) 55.
- [20] W. M. Zhang, T. Meier, V. Chernyak, S. Mukamel, *J. Chem. Phys.* 108 (1998) 7763.
- [21] M. Yang, G. R. Fleming, *Chem. Phys.* 275 (2002) 355.
- [22] T. Renger, R. A. Marcus, *J. Chem. Phys.* 107 (2003) 8404.
- [23] H. Sumi, *J. Phys. Chem. B* 103 (1999) 252.
- [24] G. D. Scholes, G. R. Fleming, *J. Phys. Chem. B* 104 (2000) 1854.
- [25] S. Jang, M. D. Newton, R. J. Silbey, *Phys. Rev. Lett.* 92 (2004) 218301.
- [26] G. Raszewski, T. Renger, *J. Am. Chem. Soc.* 130 (2008) 4431.
- [27] T. Renger, I. Trostmann, C. Theiss, M. E. Madjet, M. Richter, H. Paulsen, H. J. Eichler, A. Knorr, G. Renger, *J. Phys. Chem. B* 111 (2007) 10487.
- [28] M. Yang, A. Damjanovic, H. M. Vaswani, G. R. Fleming, *Biophys. J.* 85 (2003) 140.
- [29] T. Renger, M. E. M., A. Knorr, F. Müh, J. Plant Physiol. 168 (2011) 1497.
- [30] T. Renger, *Phys. Rev. Lett.* 93 (2004) 188101.
- [31] V. May, O. Kühn, *Charge and Energy Transfer Dynamics in Molecular Systems: A Theoretical Introduction*, Wiley-VCH, Berlin, 2000.
- [32] J. Pieper, J. Voigt, G. J. Small, *J. Phys. Chem. B* 103 (1999) 2319.
- [33] J. Adolphs, T. Renger, *Biophys. J.* 91 (2006) 2778.
- [34] C. Curutchet, G. D. Scholdes, B. Mennucci, R. Cammi, *J. Phys. Chem. B* 111 (2007) 13253.
- [35] J. Adolphs, F. Müh, M. E. Madjet, T. Renger, *Photosynth. Res.* 95 (2008) 197.
- [36] R. S. Knox, B. Q. Spring, *Photochem. Photobiol.* 77 (2003) 497.
- [37] J. Adolphs, F. Müh, M. E. Madjet, M. Schmidt am Busch, T. Renger, *J. Am. Chem. Soc.* 132 (2010) 3331.
- [38] F. Müh, M. E. Madjet, T. Renger, *J. Phys. Chem. B* 114 (2010) 13517.
- [39] F. Müh, M. E. Madjet, J. Adolphs, A. Abdurahman, B. Rabenstein, H. Ishikita, E.-W. Knapp, T. Renger, *Proc. Natl. Acad. Sci. USA* 104 (2007) 16862.
- [40] J. Eccles, B. Honig, *Proc. Natl. Acad. Sci. USA* 80 (1983) 4959.
- [41] A. Damjanovic, I. Kosztin, U. Kleinekathöfer, K. Schulten, *Phys. Rev. E* 65 (2002) 031919.
- [42] G. Fowler, R. Visschers, G. Grief, R. van Grondelle, C. Hunter, *Nature* 355 (1992) 848.
- [43] H. Witt, E. Schlodder, C. Teutloff, J. Niklas, E. Bordignon, D. Carbonera, S. Kohler, A. Labahn, W. Lubitz, *Biochemistry* 41 (2002) 8557–8569.
- [44] E. Gudowska-Nowak, M. D. Newton, J. Fajer, *J. Phys. Chem.* 94 (1990) 5795.
- [45] B. A. Diner, E. Schlodder, P. J. Nixon, W. J. Coleman, F. Rappaport, J. Lavergne, W. F. J. Vermaas, D. A. Chisholm, *Biochemistry* 40 (2001) 9265.
- [46] S. Yin, M. G. Dahlbom, P. J. Canfield, N. S. Hush, R. Kobayashi, J. R. Reimers, *J. Phys. Chem. B* 111 (2007) 9923.
- [47] R. M. Pearlstein, *Photosynth. Res.* 31 (1992) 213.
- [48] D. Gülen, *J. Phys. Chem.* 100 (1996) 17683.
- [49] R. J. W. Louwe, J. Vrieze, A. J. Hoff, T. J. Aartsma, *J. Phys. Chem. B* 101 (1997) 11280.
- [50] M. Wendling, M. A. Przyjalowski, D. Gülen, S. I. E. Vulto, T. J. Aartsma, R. van Grondelle, H. van Amerongen, *Photosynth. Res.* 71 (2002) 99.
- [51] M. Byrdin, P. Jordan, N. Krauss, P. Fromme, D. Stehlik, E. Schlodder, *Biophys. J.* 83 (2002) 433.
- [52] B. Brüggemann, K. Sznee, V. Novoderezhkin, R. van Grondelle, V. May, *J. Phys. Chem. B* 108 (2004) 13536.
- [53] G. Raszewski, W. Saenger, T. Renger, *Biophys. J.* 88 (2005) 986.
- [54] V. I. Novoderezhkin, J. P. Dekker, R. Van Grondelle, *Biophys. J.* 93 (2007) 1293.
- [55] M. E. Madjet, A. Abdurahman, T. Renger, *J. Phys. Chem. B* 110 (2006) 17268.
- [56] A. Damjanovic, H. M. Vaswani, P. Fromme, G. R. Fleming, *J. Phys. Chem. B* 106 (2002) 10251.
- [57] M. Schmidt am Busch, F. Müh, E. M. Madjet, T. Renger, *J. Phys. Chem. Lett.* 2 (2011) 93.
- [58] C. J. Law, R. J. Cogdell, in: R. G. (Ed.), *Primary Processes of Photosynthesis - Part 1, Principles and Apparatus*, RCS Publishing, Cambridge, 2008, p. 205.

- [59] A. Warshel, W. W. Parson, *J. Am. Chem. Soc.* 109 (1987) 6143–6152.
- [60] D. L. Dexter, *J. Chem. Phys.* 21 (1953) 836.
- [61] R. D. Harcourt, K. P. Ghiggino, G. D. Scholes, S. Speiser, *J. Chem. Phys.* 105 (1996) 1897.
- [62] G. Scholes, I. Gould, R. Cogdell, G. Fleming, *J. Phys. Chem. B* 103 (1999) 2543.
- [63] M. E. Madjet, F. Müh, T. Renger, *J. Phys. Chem. B* 113 (2009) 12603.
- [64] S. G. Boxer, T. R. Middendorf, D. J. Lockhart, *FEBS Lett.* 200 (1986) 237.
- [65] P. Lyle, S. V. Kolaczowski, G. J. Smal, *J. Phys. Chem.* 97 (1993) 6924.
- [66] H. Huber, M. Meyer, H. Scheer, W. Zinth, J. Wachtveitl, *Photosynth. Res.* 55 (1998) 153.
- [67] E. J. P. Lathrop, R. A. Friesner, *J. Phys. Chem.* 98 (1994) 3056.
- [68] H. Zhou, S. G. Boxer, *J. Phys. Chem. B* 101 (1997) 5759.
- [69] U. Fano, *Phys. Rev.* 124 (1961) 1866.
- [70] S. Mukamel, I. Oppenheim, J. Ross, *Phys. Rev. A* 17 (1978) 1988.
- [71] T. Renger, R. A. Marcus, *J. Chem. Phys.* 116 (2002) 9997.
- [72] D. E. Tronrud, M. F. Schmid, B. W. Matthews, *J. Mol. Biol.* 188 (1986) 443–454.
- [73] H. W. Rémy, H. Stahlberg, D. Fotiadis, B. Wolpensinger, A. Engel, G. Hauska, G. Tsiotis, *J. Mol. Biol.* 290 (1999) 851–858.
- [74] A. N. Melkozernov, J. M. Olson, Y. F. Li, J. P. Allen, R. E. Blankenship, *Photosynth. Res.* 56 (1998) 315.
- [75] J. Wen, H. Zhang, M. L. Gross, R. E. Blankenship, *Proc. Natl. Acad. Sci. USA* 106 (2009) 6134–6139.
- [76] A. BenShem, F. Frolow, N. Nelson, *FEBS Lett.* 564 (2004) 274.
- [77] D. E. Tronrud, J. Wen, L. Gay, R. E. Blankenship, *Photosynth. Res.* 100 (2009) 79–87.
- [78] G. S. Engel, T. R. Calhoun, E. L. Read, T. K. Ahn, T. Mancal, Y. C. Cheng, R. E. Blankenship, G. R. Fleming, *Nature* 446 (2007) 782.
- [79] Z. F. Liu, H. C. Yan, K. B. Wang, T. Y. Kuang, J. P. Zhang, L. L. Gui, X. M. An, W. R. Chang, *Nature* 428 (2004) 287.
- [80] J. Standfuss, A. C. Terwisscha van Scheltinga, M. Lamborghini, W. Kühlbrandt, *EMBO J.* 24 (2005) 919.
- [81] V. I. Novoderezhkin, M. A. Palacios, H. van Amerongen, R. van Grondelle, *J. Phys. Chem. B* 109 (2005) 10493.
- [82] H. M. Visser, F. J. Kleima, I. H. M. van Stokkum, R. van Grondelle, H. van Amerongen, *Chem. Phys.* 210 (1996) 297.
- [83] F. J. Kleima, C. C. Gradinaru, F. Calkoen, I. H. M. van Stokkum, R. van Grondelle, H. van Amerongen, *Biochemistry* 36 (1997) 15262.
- [84] C. C. Gradinaru, S. Özdemir, D. Gülen, I. H. M. van Stokkum, R. van Grondelle, H. van Amerongen, *Biophys. J.* 75 (1998) 3064.
- [85] R. Remelli, C. Varotto, D. Sandona, R. Croce, R. Bassi, *J. Biol. Chem.* 274 (1999) 33510.
- [86] H. Rogl, R. Schödel, H. Lokstein, W. Külbrandt, A. Schubert, *Biochemistry* 41 (2002) 2281.
- [87] P. W. Hemelrijk, S. L. S. Kwa, R. van Grondelle, J. P. Dekker, *Biochim. Biophys. Acta* 1098 (1992) 159.
- [88] J. Pieper, M. Rätsep, R. Jankowiak, K. D. Irrgang, J. Voigt, G. Renger, G. J. Small, *J. Phys. Chem. A* 103 (1999) 2412.
- [89] G. S. Schlau-Cohen, T. R. Calhoun, N. Ginsberg, E. L. Read, M. Ballottari, R. Bassi, R. van Grondelle, G. R. Fleming, *J. Phys. Chem. B* 113 (2009) 16291.
- [90] G. S. Schlau-Cohen, T. R. Calhoun, N. Ginsberg, M. Ballottari, R. Bassi, G. R. Fleming, *Proc. Natl. Acad. Sci. USA* 107 (2010) 13267.